



## RESEARCH ARTICLES

### Effect of Self-Association of Phenol on Its Transport across Polyethylene Film

T. J. MIKKELSON <sup>‡</sup>, S. WATANABE <sup>\*</sup>, J. H. RYTTING, and T. HIGUCHI

Received July 30, 1979, from the *Department of Pharmaceutical Chemistry, University of Kansas, Lawrence, KS 66044*. Accepted for publication September 10, 1979. <sup>\*</sup>Present address: Eisai Co. Ltd., Tokyo, Japan.

**Abstract** □ Phenol diffusion across a high density polyethylene film from isooctane, in which phenol self-associates, demonstrated nonideal behavior. The steady-state flux of phenol across the film was not directly proportional to its concentration in the donor phase. At higher donor phase concentrations, negative steady-state flux deviations were observed. These negative deviations were due to phenol self-association in the donor phase and the resulting decreases in thermodynamic activity. By using a monomer-pentamer model for phenol self-association in isooctane, the steady-state flux was shown to be directly proportional to the phenol monomer concentration in the donor phase. Although steady-state flux concentration deviations were observed, the diffusion time lag was independent of the permeant concentration and reflected the intrinsic diffusivity of the film to phenol.

**Keyphrases** □ Phenol—effect of self-association on transport across polyethylene film □ Self-association—phenol, effect on transport across polyethylene film □ Mass transfer—phenol self-association, effect on membrane transport □ Diffusion—phenol self-association, effect on membrane transport □ Flux, steady state—effect of phenol self-association on transport across polyethylene film

Mass transfer processes in drug delivery include those that are involved in drug release from a dosage unit and those that are involved in drug transport across biological membranes. The rate and extent of these processes depend on the film or absorbing membrane, the physicochemical characteristics of the permeating drug, and the properties of the drug delivery unit. The dependency of these mass transfer processes on physicochemical drug properties and membrane characteristics has been extensively studied because it is an integral part of drug research and development. Determinants such as molecular size, crystalline form, solubility, pH and ionization, charge, complexation, and partitioning have been identified and continue to be characterized relative to their significance.

There is continuing interest in these laboratories in the effects of specific molecular interactions in solution. For example, many molecules with polar functional groups undergo pronounced self-association in nonpolar solvent

systems, resulting in changes in thermodynamic activity (1-3).

The properties of alcohols in hydrocarbon solvents have been studied extensively. Self-association is a dominant factor in the lower than expected vapor pressures of alcohols (1-3). The anomalous solubility behavior of phenol in hydrocarbon solvents is a function of self-association (3). Furthermore, dissolution characteristics of an alcohol deviating from a modified Noyes-Whitney prediction (4) can be rationalized on the basis of self-association.

This report describes specifically the effects of phenol self-association in isooctane on phenol transport across a high density polyethylene film. The effect of self-association on transport was described previously only in general and descriptive terms (5-7). This report describes quantitatively the changes in transport properties resulting from the self-association of a permeating species in the donor phase of a diffusion assembly in terms of an exact molecular association model.

#### THEORETICAL

**Steady-State Permeation**—Fick's first law was formulated as:

$$J = -D \left( \frac{dC}{dx} \right) \quad (\text{Eq. 1})$$

where  $J$  is the flux of material across a unit area of film,  $D$  is the diffusion coefficient, and  $(dC/dx)$  is the concentration differential across the film. The negative sign implies that the material flow is from an element of higher concentration to an element of lower concentration. For an isotropic or homogeneous film of a given cross-sectional area and a constant thickness, Fick's law can be expressed as:

$$J = PA \Delta C \quad (\text{Eq. 2})$$

where  $J$  is the net flux of material or the appearance of permeant on the receptor side,  $P$  is the permeability coefficient,  $A$  is the cross-sectional area of the film or membrane, and  $\Delta C$  is the concentration difference across the total film thickness.

Under sink conditions,  $\Delta C$  is replaced with the concentration of permeant in the donor phase,  $C_d$ , and the permeability coefficient or permeability,  $P$ , becomes:

$$P = \frac{D_m K}{h_m} \quad (\text{Eq. 3})$$

where  $D_m$  is the permeant diffusivity or diffusion coefficient in the membrane,  $K$  is the membrane-donor phase partition coefficient, and  $h_m$  is the membrane thickness. This development assumes a partition-diffusion mass transfer mechanism, in contrast to a pore permeation mechanism. A partition-diffusion mechanism has been demonstrated for polyethylene films and the transport of numerous solute materials of general and pharmaceutical interest (8-10).

From measurements of the permeant concentration appearing in the receptor phase as a function of time, the parameters descriptive of the transfer process can be obtained readily, in part from the steady-state permeation. By utilizing the expression:

$$J = \frac{dQ}{dt} = V \left( \frac{dC}{dt} \right) \quad (\text{Eq. 4})$$

(where  $Q$  is the amount of permeant reaching the receptor site,  $V$  is the volume of the receptor phase or compartment, and  $C$  is the permeant concentration reaching the receptor side), and combining it with the expression  $\Delta C = C_d$  and with Eq. 2, the result is:

$$\frac{V}{A} \left( \frac{dC}{dt} \right) = PC_d \quad (\text{Eq. 5})$$

In a steady-state experiment, where  $C_d$  remains essentially unchanged (*i.e.*, where the amount of permeant transported or the concentration of permeant achieved in the receptor phase is small compared to  $C_d$ ), a plot of  $C$  versus  $t$  following an initial time lag will be linear. From the slope,  $dC/dt$ , of the linear portion of the plot, the steady-state flux,  $SSF$ , is obtained by:

$$SSF = \frac{V}{A} \left( \frac{dC}{dt} \right) \quad (\text{Eq. 6})$$

which, in turn, results in:

$$SSF = PC_d \quad (\text{Eq. 7})$$

allowing for the determination of permeability by:

$$P = \frac{SSF}{C_d} \quad (\text{Eq. 8})$$

Equations 6 and 8 provide a means of computing the steady-state flux and permeability from observed data obtained in a steady-state experiment. Further system elucidation is achieved by defining and solving the permeability coefficient,  $P$ , which is a function of the diffusion coefficient of the permeant in the membrane,  $D_m$ , the thickness of the membrane,  $h_m$ , and the membrane-donor phase partition coefficient,  $K$ . The contribution of the partition coefficient to permeability results from use of the donor phase concentration as a reference to the actual concentration of the permeant in the membrane at the donor phase-membrane interface. The relationship is presented in Eq. 3. Of these three parameters ( $D_m$ ,  $h_m$ , and  $K$ ), only the  $h_m$  term, which is experimentally defined, is known. To obtain values of  $D_m$  and  $K$ , one of them must be independently determined; evaluation of the nonsteady-state data from the same experiments permits the calculation of  $D_m$ . Therefore, to elucidate the mass transfer process taking place, an analysis of nonsteady-state permeation is used.

**Nonsteady-State Permeation**—The necessary equation for determining the diffusivity,  $D_m$ , from the nonsteady-state permeation characteristics across an isotropic or homogeneous film was reported (11) and is:

$$t_L = \frac{h_m^2}{6D_m} \quad (\text{Eq. 9})$$

where  $t_L$  is the diffusion time lag. From Eq. 9, it can be seen that, for a homogeneous film, the time lag is a function only of the membrane thickness and the membrane diffusivity. The time lag is obtained by extrapolation of the linear steady-state data back to its time axis intercept. As a result, for a membrane of known thickness, the membrane diffusivity can be computed. With this information, the membrane-donor phase partition coefficient can be computed using Eq. 3.

**Self-Association**—The mass transfer characteristics of a self-associating permeant may demonstrate nonideal behavior when interpreted directly through Fick's laws. The nonideal behavior arises from a dependency on the effective concentration (thermodynamic activity or

chemical potential) of the permeant, rather than the total concentration, and/or a dependency on the effective diffusion coefficient, which changes as a function of the size of the associated species and the extent of its formation. The contribution of self-association to a particular mass transfer process depends on the experimental conditions. Self-association can potentially occur in the phases contacting a membrane, such as the donor phase, and/or within the membrane itself, depending on donor phase and membrane characteristics.

For a nonassociating permeant diffusing through a homogeneous membrane in the steady state, Eq. 1 is directly applicable. For this simple system, the activity or concentration gradient across the film is linear.

For a system of a self-associating solute diffusing through a homogeneous membrane, Eq. 1 is not directly applicable. If it is assumed that this self-association is an equilibrium between a monomer and a single polymer species, there exists a gradient of each species, monomer and polymer, across the film, and the reaction between them will be at equilibrium within all elements within the film. As a result, the gradients of the two species across the film are nonlinear.

Approaches to quantitating the system can be empirical or modelistic. In the empirical approach, the total flux of permeant (monomer and polymer) can be described in terms of an observed or apparent diffusion coefficient, which is concentration dependent. Such an approach was suggested by Barrer (12); the equation for the diffusivity relates diffusivity to concentration:

$$D = BRT \frac{d \ln a}{d \ln c} \quad (\text{Eq. 10})$$

where  $R$  and  $T$  have their usual meaning,  $a$  is activity, and  $B$  is a coefficient reflecting the mobility of the permeant. Barrer (12) pointed out that both  $B$  and  $(d \ln a / d \ln c)$  can depend on permeant concentration. Such an approach was taken by Longworth (5), who interpreted the mass transfer of self-associating acids and alcohols in carbon tetrachloride in terms of an apparent diffusion coefficient, which decreases as a function of increasing total permeant concentration.

Under experimental conditions where permeant self-association occurs in the donor phase but only the monomeric species diffuses across the film, the observed nonideal characteristics of transport are explained in terms of effective concentration or chemical potential of permeant in the donor phase. This type of system is being reported here. The experimental results indicate that only the phenol monomer is transported across the polyethylene film and that the intrinsic membrane permeability remains unchanged. However, over the donor concentrations studied, phenol self-association in the isooctane donor phase, which decreases the effective donor phase concentration or activity of the permeant, appreciably influences mass transfer.

The literature affords significant data on the self-association of alcohols and its effect on vapor pressure (1, 2), spectral properties (13), solubility (3), and transport characteristics from an empirical standpoint (5). The effect of donor phase self-association on permeation characteristics across a membrane can be more systematically described by incorporation of a model describing the donor phase self-association rather than interpretation of experimental results in terms of a changing apparent or observed diffusion coefficient.

Phenol self-association in isooctane and cyclohexane has been studied in detail (3). These systems are adequately described in terms of a monomer-pentamer model. Given the information that a monomer-pentamer model is appropriate ( $n = 5$ ) and given the equilibrium or association constant,  $K_{1,5}$ , monomer concentrations for a given total concentration can be calculated.

**Permeation Model**—The system of a solute that self-associates in a donor solvent but permeates a membrane only in its monomer form can be described by extending Eq. 7 to account for self-association. This system is diagrammed in Scheme I. A mathematical description of Scheme I is given in the following two equations:

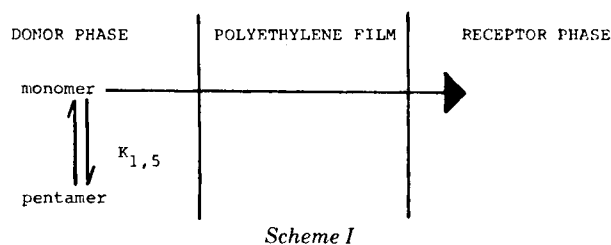
$$SSF = PC_{\text{mon}} \quad (\text{Eq. 11})$$

$$SSF = \left( \frac{D_m K}{h_m} \right) C_{\text{mon}} \quad (\text{Eq. 12})$$

where  $P$  is the intrinsic membrane permeability and  $K$  is the intrinsic membrane-donor phase partition coefficient. These equations relate the steady-state flux to the monomer concentration of permeant in the donor phase. The expression  $C_{\text{mon}} = (f_{\text{mon}})(C_T)$  allows Eq. 11 to be written as:

$$SSF = (P_{\text{obs}})(C_T) \quad (\text{Eq. 13})$$

where  $P_{\text{obs}}$  is the observed permeability and is related to the other pa-



rameters by  $P_{obs} = (D_m K / h_m)(f_{mon})$ . This relationship indicates that the observed permeability is equal to the product of the intrinsic permeability and the monomer fraction of permeant in the donor phase,  $P_{obs} = P f_{mon}$ . This approach allows the system to be interpreted in terms of an observed permeability.

The system can also be interpreted in terms of an apparent or observed partition coefficient,  $K_{obs}$ . This approach results in:

$$SSF = \left( \frac{D_m}{h_m} \right) (K_{obs})(C_T) \quad (\text{Eq. 14})$$

where  $K_{obs} = K f_{mon}$ .

This approach, beginning with Eq. 13, allows studies (permeant self-association in the donor phase, but membrane transport of only the monomer species) to be described in terms of an observed permeability or an observed partition coefficient when the reference concentration parameter is the total permeant concentration,  $C_T$ , in the donor phase. However, the most precise description is in terms of the intrinsic parameters, the intrinsic permeability,  $P$ , and the intrinsic partition coefficient,  $K$ , and by fully describing the donor phase self-association in terms of  $n$  and  $K_{1,n}$ .

The system can be resolved partially using only permeation data, without precise knowledge of the self-association equilibrium. The full mathematical expression for the system in terms of permeation is:

$$SSF = \left( \frac{D_m K}{h_m} \right) (f_{mon})(C_T) \quad (\text{Eq. 15})$$

From each experiment in a series of permeation experiments,  $SSF$  is determined as a function of  $C_T$ . Since the membrane thickness,  $h_m$ , is defined experimentally, the measured diffusion time lags permit calculation of  $D_m$  using Eq. 9;  $K$  and  $f_{mon}$  remain unsolved. However,  $K$  can be obtained by proper experimental design. Since  $f_{mon}$  goes to unity at low concentrations, experimental runs at low concentrations, where the self-association is negligible, allow determination of  $K$ ; i.e.,  $K_{obs} = K$  as  $f_{mon}$  goes to unity. As a result, experiments conducted at higher  $C_T$  can be interpreted in terms of  $f_{mon}$ ,  $P$ , and  $K$  using the information obtained from the experiments conducted at low concentrations.

The approach of resolving the system only from interpretation of permeation data permits an estimation of  $f_{mon}$ , which is, however, a general description of the self-association. An accurate and complete understanding of the processes, both permeation and self-association, is best provided by a direct and independent equilibrium determination of  $C_{mon}$  as a function of  $C_T$ , such that  $n$  and  $K_{1,n}$  are precisely known. For the phenol-isooctane mixtures used as the donor phases in this study, the values of  $n$  and  $K_{1,n}$  were measured independently (3). This information permitted the processes to be more readily interpreted and modeled by providing independent verification of the experimental results.

## EXPERIMENTAL

**Materials**—High density polyethylene films<sup>1</sup> were used. Phenol<sup>2</sup>, analytical reagent grade, was used without further purification. The isooctane<sup>3</sup> had a labeled purity of 99+ mole %. It was stored over a molecular sieve and otherwise used as received. All other chemicals were analytical reagent grade.

**Analytical Method**—All phenol concentrations were determined by direct spectrophotometric<sup>4</sup> measurement at 269 nm ( $\log \epsilon = 3.18$ ) in 0.1 M aqueous sulfuric acid.

**Diffusion Cells**—Pyrex glass diffusion cells were constructed. They consisted of identical cylindrical half-cells between which the polyethylene film was mounted. The half-cell chambers were slightly tapered

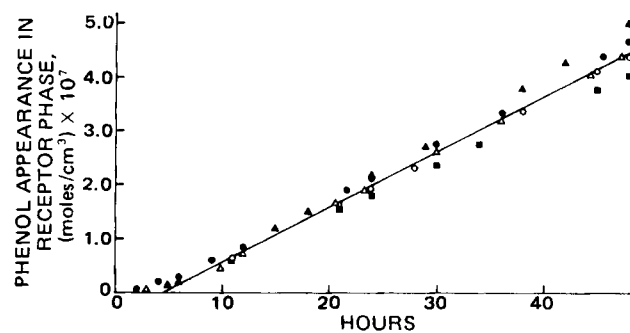


**Figure 1**—Phenol concentration appearing in the receptor phase as a function of time. The donor phase phenol concentration was  $2.00 \times 10^{-4}$  mole/cm<sup>3</sup>. The different symbols represent five individual experiments. The drawn line is that obtained by linear regression analysis of the data points for times equal to or greater than 15 hr from all five individual experiments.

and had a mean inside diameter of approximately 5.5 cm and an inside height or depth of approximately 6.0 cm, resulting in a half-cell volume of 145 ml. Each half-cell was constructed with a cylindrical portal extending off the cylinder side, allowing for filling of the compartments and withdrawing of samples. The open or contact end of the half-cells was of ground glass and grooved to accept an O-ring. The sequence of half-cell-O-ring-polyethylene membrane-O-ring-half-cell was firmly maintained using a metal clamp.

The assembled cell was immersed in a well-stirred constant-temperature bath, and the contents were well stirred by positioning magnetic stirrers directly below the half-cells beneath the water bath. Rapid mixing and homogeneity of the half-cell solutions were verified visually by use of a dye.

The cross-sectional area of the membrane over which the transport occurred was 29.7 cm<sup>2</sup>, which resulted in an area to volume ratio of 0.20 cm<sup>-1</sup>.

**Diffusion Study**—Prior to assembly, the polyethylene films were soaked to an equilibrium swelling in isooctane. The swelled film thickness was determined to be  $0.078 \pm 0.002$  cm using a screw micrometer graduated to 0.001 cm.

Following assembly, the cell was immersed in a constant-temperature bath maintained at  $25.0 \pm 0.1^\circ$ . The receptor compartment was filled with 145 ml of an aqueous solution of 0.1 M H<sub>2</sub>SO<sub>4</sub>. The donor compartment was filled with 145 ml of the test solutions of phenol in isooctane. The stir bars were immediately rotated at greater than 200 rpm, which commenced the experiment. This degree of stirring ensured membrane, and not diffusion layer, rate-limited transport.

At preselected intervals, 1.0-ml samples were withdrawn from the receptor compartment and immediately analyzed spectrophotometrically for phenol. The receptor compartment volume was maintained at 145 ml by addition of 1.0 ml of 0.1 M H<sub>2</sub>SO<sub>4</sub> following sample removal. Aqueous sulfuric acid was used as the receptor phase to facilitate the analytical measurement for greater chemical stability and to suppress phenol ionization.

## RESULTS AND DISCUSSION

Permeation studies were conducted at 12 donor phase concentrations of phenol in isooctane over  $0.05$ – $2.00 \times 10^{-4}$  mole/cm<sup>3</sup>. Figure 1, a plot of the phenol concentration in the receptor phase as a function of time, shows the data from five runs using a donor phase concentration of  $2.0 \times 10^{-4}$  mole/cm<sup>3</sup>. The linear steady-state portion and the time lag, which are typical of an experiment conducted under sink conditions with a constant donor phase concentration, are evident.

From the data obtained at each donor phase concentration, the steady-state flux was determined from the slope of the linear portion of the curve using Eq. 6 and linear regression data analysis. Since the experimental time lags were approximately 5 hr at each donor phase concentration, only data obtained at times greater than 15 hr were used in calculating the steady-state flux values. The line drawn in Fig. 1 is the regression line and corresponds to a steady-state flux of  $1.36 \times 10^{-11}$  mole/sec/cm<sup>2</sup>. The 32 data points obtained at 15 hr or longer from the five experiments gave a correlation coefficient of 0.987. Extrapolation of the regression line to the time axis resulted in a time lag of 4.6 hr.

The steady-state flux and the extrapolated time lag,  $t_L$ , values calculated for the 12 donor phase concentrations are given in Table I. Figure

<sup>1</sup> Cadillac Plastic and Chemical Co., Kansas City, Kans.

<sup>2</sup> Mallinckrodt Chemical Works.

<sup>3</sup> Phillips Petroleum Co.

<sup>4</sup> Cary model 118 spectrophotometer, Varian Instrument Division.

**Table I—Experimentally Observed Steady-State and Nonsteady-State Diffusion Parameters of Phenol across High Density Polyethylene Film for the Phenol Concentrations Studied**

| $C_T^a$ ,<br>(moles/cm <sup>3</sup> )<br>× 10 <sup>4</sup> | $q^b$ | $m^c$ | $SSF^d$ ,<br>(moles/sec/cm <sup>2</sup> )<br>× 10 <sup>11</sup> | $r^e$ | $t_L^f$ ,<br>hr |
|--|-------|-------|---|-------|-----------------|
| 2.00   | 5     | 32    | 1.36  | 0.987 | 4.6             |
| 1.75   | 6     | 41    | 1.22  | 0.976 | 5.2             |
| 1.50   | 6     | 41    | 1.17  | 0.983 | 5.2             |
| 1.25   | 5     | 33    | 1.17  | 0.990 | 5.4             |
| 1.00   | 5     | 32    | 1.02  | 0.969 | 5.1             |
| 0.75   | 5     | 34    | 0.853   | 0.982 | 4.9             |
| 0.50   | 5     | 34    | 0.676   | 0.972 | 5.0             |
| 0.25   | 3     | 21    | 0.396   | 0.993 | 5.3             |
| 0.20   | 3     | 21    | 0.331   | 0.985 | 5.3             |
| 0.15   | 3     | 21    | 0.234   | 0.973 | 5.2             |
| 0.10   | 3     | 21    | 0.165   | 0.974 | 5.1             |
| 0.05   | 3     | 21    | 0.079   | 0.987 | 5.8             |
|  |       |       |   |       | $\bar{M} = 5.2$ |
|  |       |       |   |       | $\sigma = 0.3$  |

<sup>a</sup> Total phenol concentration in the donor phase. <sup>b</sup> Number of experimental runs. <sup>c</sup> Number of individual data points used in the calculation of the steady-state flux. <sup>d</sup> Steady-state flux. <sup>e</sup> Correlation coefficient using  $m$  data points. <sup>f</sup> Time lag of diffusion.

2a shows the steady-state permeation data given in Table I, where the calculated steady-state flux values are plotted as a function of the total phenol concentration in the donor phase. This plot is linear at low donor phase concentrations up to  $\sim 0.25 \times 10^{-4}$  mole/cm<sup>3</sup>. At donor phase

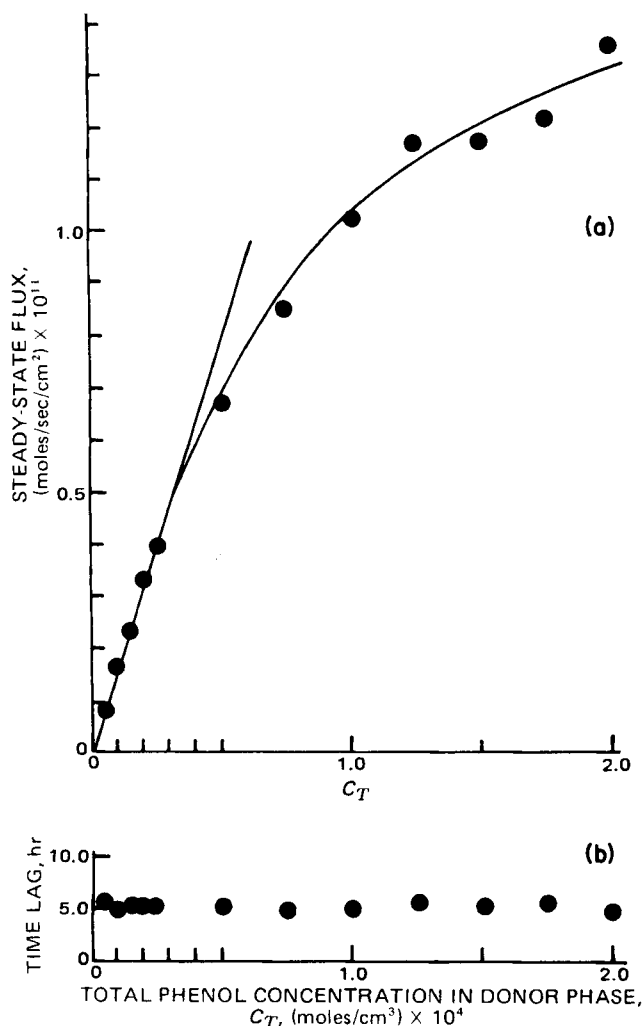


**Figure 2—(a) Steady-state flux as a function of the total phenol concentration in the donor phase. (b) Observed diffusion time lag as a function of the total phenol concentration in the donor phase.**

**Table II—Phenol Monomer Concentrations and Fractions, Observed Permeabilities, and Observed Partition Coefficients for the Phenol Concentrations Studied**

| $C_T^a$ ,<br>(moles/cm <sup>3</sup> )<br>× 10 <sup>4</sup> | $C_{mon}^b$ ,<br>(mole/cm <sup>3</sup> )<br>× 10 <sup>4</sup> | $f_{mon}^c$ | $P_{obs}^d$ ,<br>(cm/sec)<br>× 10 <sup>8</sup> | $K_{obs}^e$       |
|--|---|-------------|--|-------------------|
| 2.0  | 0.82  | 0.41        | 6.8  | 0.09              |
| 1.75   | 0.79  | 0.45        | 6.9  | 0.10              |
| 1.50   | 0.75  | 0.50        | 7.8  | 0.11              |
| 1.25   | 0.71  | 0.57        | 9.3  | 0.14              |
| 1.00   | 0.65  | 0.65        | 10.2   | 0.14              |
| 0.75   | 0.57  | 0.76        | 11.4   | 0.16              |
| 0.50   | 0.44  | 0.88        | 13.5   | 0.19              |
| 0.25   | 0.25  | 1.00        | 15.9 <sup>f</sup>                              | 0.23 <sup>g</sup> |
| 0.20   | 0.20  | 1.00        | 16.5 <sup>f</sup>                              | 0.24 <sup>g</sup> |
| 0.15   | 0.15  | 1.00        | 15.6 <sup>f</sup>                              | 0.23 <sup>g</sup> |
| 0.10   | 0.10  | 1.00        | 16.5 <sup>f</sup>                              | 0.23 <sup>g</sup> |
| 0.05   | 0.05  | 1.00        | 15.9 <sup>f</sup>                              | 0.25 <sup>g</sup> |
|  |   |             | $M = 16.1$                                     | $M = 0.24$        |
|  |   |             | $\sigma = 0.4$                                 | $\sigma = 0.01$   |

<sup>a</sup> Total phenol concentration in the donor phase. <sup>b</sup> Concentration of phenol monomer in the donor phase. <sup>c</sup> Fraction of phenol monomer in the donor phase. <sup>d</sup> Experimentally observed permeability. <sup>e</sup> Experimentally observed membrane-donor phase partition coefficient. <sup>f</sup> The  $P_{obs}$  values used to calculate the mean value of  $16.1 \times 10^{-8}$  cm/sec. <sup>g</sup> The  $K_{obs}$  values used to calculate the mean value of 0.24.

concentrations greater than  $0.25 \times 10^{-4}$  mole/cm<sup>3</sup>, a negative deviation from linearity is observed, which increases in severity at larger values of  $C_T$ .

The time lags,  $t_L$ , at each donor phase concentration (Table I) are plotted in Fig. 2b as a function of  $C_T$ . The time lag is seen to be independent of the donor phase permeant concentration. An averaged value of the time lag computed from the experiments at the 12 donor phase concentrations is  $5.2 \pm 0.3$  hr. By using this value and applying Eq. 9, the membrane diffusion coefficient for phenol was found to be  $5.4 \times 10^{-8}$  cm<sup>2</sup>/sec.

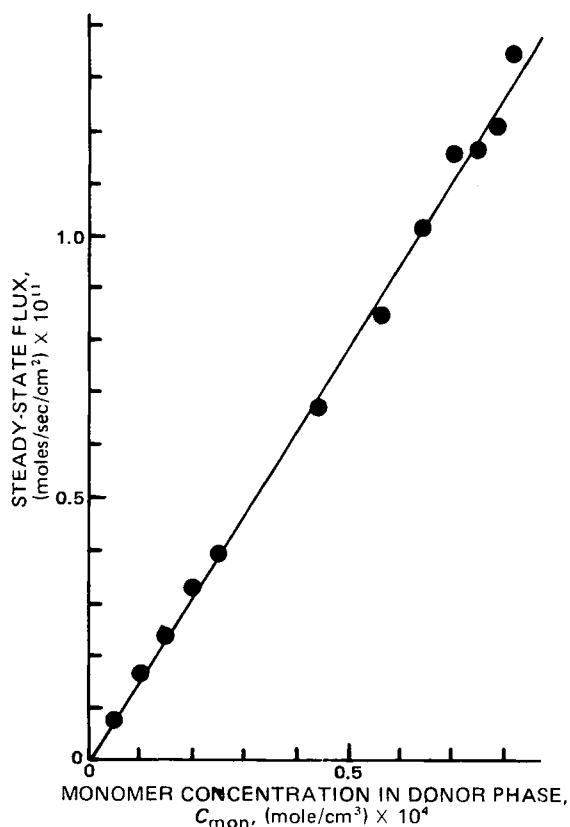


**Figure 3—Steady-state flux as a function of the donor phase phenol monomer concentration. The slope of the line, which was obtained by regression analysis, equals  $15.9 \times 10^{-8}$  cm/sec and represents the intrinsic permeability of the film to phenol contained in a donor phase of isoctane.**

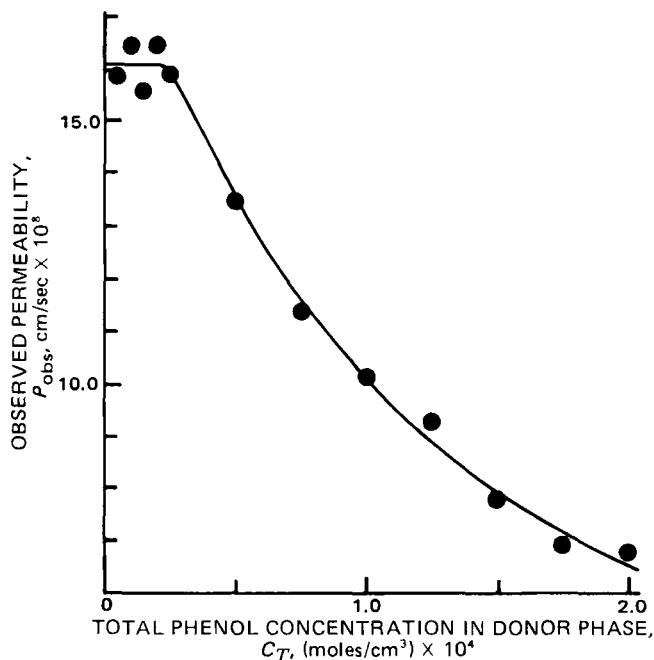


Figure 4—Observed permeability coefficients as a function of the total phenol concentration in the donor phase.

Ideally, these experiments would conform with Eq. 7, which predicts linearity in a plot of steady-state flux against donor phase concentration. The resulting slope would equal membrane permeability. Equation 7 is an expression of Fick's first law and includes the term  $C_d$ , the concentration difference across the film, which is typically taken to be the driving force for diffusion. However, as pointed out by Flynn *et al.* (14), the fundamental flux determinant is the chemical potential difference across the film. The nonlinearity actually observed was accounted for by relating the steady-state flux to the concentration gradient of the phenol monomer rather than to its total concentration.

With recently published data (3) on phenol self-association, the phenol monomer concentration in the isoctane donor solutions was calculated using an association constant,  $K_{1,5}$ , of  $6.26 \times 10^3$  liters<sup>4</sup>/mole<sup>4</sup>. These concentrations and the fraction of phenol monomer,  $f_{mon}$ , are given in Table II. In the concentrations studied, the phenol exists totally as a monomer (negligible self-association) at or below  $0.25 \times 10^{-4}$  mole/cm<sup>3</sup>.

A plot of the steady-state flux as a function of the donor phase concentration of the phenol monomer,  $C_{mon}$ , is presented in Fig. 3. The figure, a plot of Eq. 11 or 12, is linear. The slope of the line equals  $15.9 \times 10^{-8}$  cm/sec (correlation coefficient of 0.998) and represents the intrinsic permeability of the polyethylene film under the experimental conditions. This slope or intrinsic permeability value obtained from Fig. 3 should be identical to the initial slope value in Fig. 2, where the total phenol concentration is plotted as the abscissa, because at the phenol concentrations corresponding to the first five data points in Fig. 2, the phenol exists in effect totally as a monomer. This can be demonstrated by two different calculations. From the initial slope in Fig. 2, generated using the paired ( $C_T$ , SSF) data points for the five lowest phenol concentrations, a permeability of  $16.0 \times 10^{-8}$  cm/sec is obtained, in comparison to the value of  $15.9 \times 10^{-8}$  cm/sec obtained from the slope in Fig. 3. Alternatively, as can be seen in Table II, the individual  $P_{obs}$  values corresponding to the five lowest phenol concentrations yield an average value of  $16.1 \times 10^{-8}$  cm/sec.

Apparent or observed permeability values,  $P_{obs}$ , were calculated from the steady-state flux values at each donor phase concentration using Eq. 13 (Table II). These  $P_{obs}$  values are plotted in Fig. 4 as a function of  $C_T$ . This plot displays the significant decline in the apparent permeability at the higher donor phase concentrations where there is significant phenol self-association. The dependence of permeation on the monomer concentration is further substantiated by comparing the observed permeabilities

to the monomer fractions. For the data in Table II, at a  $C_T$  of  $2.00 \times 10^{-4}$  mole/cm<sup>3</sup>, the monomer fraction is 0.41. By comparison, the  $P_{obs}$  is  $6.8 \times 10^{-8}$  cm/sec, 0.43 times the value of  $15.9 \times 10^{-8}$  cm/sec obtained from the slope of Fig. 3. Similarly, at a  $C_T$  of  $1.00 \times 10^{-4}$  mole/cm<sup>3</sup>, the monomer fraction is 0.65. In comparison, the  $P_{obs}$  is  $10.2 \times 10^{-8}$  cm/sec, 0.64 times the Fig. 3 slope value.

The data in Fig. 2a indicate that permeant self-association decreases the ability of the phenol to undergo transport across the polyethylene film. At total phenol concentrations greater than  $0.25 \times 10^{-4}$  mole/cm<sup>3</sup>, there is not a proportionate increase in its steady-state flux across the polyethylene film. However, these steady-state flux data do not indicate whether the self-association effect is restricted only to the level of the donor phase or also occurs within the membrane.

An interpretation of the nonsteady-state data provides insight into the location of the self-association effect. As is evident in Fig. 2b, the experimentally determined time lags are independent of the donor phase phenol concentration, which indicates that the membrane diffusion coefficient is concentration independent. If permeant self-association occurred within the membrane, it would occur to an increasing extent as the donor phase permeant concentration increased. This increasing occurrence in the membrane of a polymer species at higher levels of  $C_T$  should increase the experimentally observed time lag. The time lag increase would result from a decrease in the effective diffusion coefficient, because of the inverse dependency of a diffusion coefficient on the effective molecular weight. However, since the diffusion coefficient is concentration independent, it can be concluded that (a) phenol self-association does not occur within the polyethylene film, or (b) if self-association is occurring within the membrane, its extent is negligible or the transport of the polymer species across the membrane is not sufficient to affect transport parameters, *i.e.*, it does not alter the diffusion coefficient.

The linearity seen in Fig. 3 suggests that the contribution of the self-association is restricted to the donor phase. Since there is an apparent direct dependency of the steady-state flux on the monomer concentration of phenol in the donor phase, it appears that only the monomer is partitioning into the membrane. This interpretation is further supported by the  $K_{obs}$  values found in Table II. The  $K_{obs}$  values, which are the experimentally observed polyethylene–isoctane partition coefficients, are closely approximated by calculating the product of the independently calculated  $f_{mon}$  values and the average intrinsic partition coefficient of 0.24, which is the observed value obtained from the experiments at the five lowest donor phase concentrations.

## REFERENCES

- (1) B. D. Anderson, J. H. Rytting, and T. Higuchi, *Int. J. Pharm.*, **1**, 15 (1978).
- (2) J. H. Rytting, B. D. Anderson, and T. Higuchi, *J. Phys. Chem.*, **82**, 2240 (1978).
- (3) B. D. Anderson, J. H. Rytting, and T. Higuchi, *J. Am. Chem. Soc.*, **101**, 5194 (1979).
- (4) T. Higuchi, S. Dayal, and I. H. Pitman, *J. Pharm. Sci.*, **61**, 695 (1972).
- (5) L. G. Longworth, *J. Colloid Interface Sci.*, **22**, 3 (1966).
- (6) I. Auerbach, W. R. Miller, W. C. Kuryla, and S. D. Gehman, *J. Polym. Sci.*, **28**, 129 (1958).
- (7) J. T. Edward, *J. Chem. Educ.*, **47**, 261 (1970).
- (8) M. Salame, *SPE Trans.*, **1961**, 153.
- (9) D. G. Serota, M. C. Meyer, and J. Autian, *J. Pharm. Sci.*, **61**, 416 (1972).
- (10) K. Nasim, M. C. Meyer, and J. Autian, *ibid.*, **61**, 1775 (1972).
- (11) R. M. Barrer, *Trans. Faraday Soc.*, **35**, 628 (1939).
- (12) R. M. Barrer, *Discuss. Faraday Soc.*, **21**, 138 (1956).
- (13) A. N. Fletcher and C. A. Heller, *J. Phys. Chem.*, **71**, 3742 (1967).
- (14) G. L. Flynn, S. H. Yalkowsky, and T. J. Roseman, *J. Pharm. Sci.*, **63**, 479 (1974).

## ACKNOWLEDGMENTS

Supported by Grant GM22357 from the National Institutes of Health.